

Nucleation and Growth of bundles of Single-Wall Carbon Nanotubes (C-SWNTs): the Bénard-Marangoni Instability (BMI) model

F.Larouche,^{1,*} J.Duquette,^{2,†} L.Cortelezzi,^{2,‡} N.Nigam,³ and B.Stansfield¹

¹*INRS, Énergie, Matériaux et Télécommunications, Canada*

²*Mechanical Engineering Department, McGill University, Canada*

³*Mathematics and Statistics Department, McGill University, Canada.*

(Dated: November 20, 2018)

A complete explanation of the synthesis of metal-catalyst nanoparticles, and the subsequent nucleation and growth of bundles of C-SWNTs is introduced using a novel model. It is shown that the synthesis process leads to the formation of a liquid layer supersaturated in carbon surrounding each metallic-catalyst nanoparticle. The onset of a solutal Bénard-Marangoni instability and the subsequent formation of patterns of hexagonal convection cells in the liquid layer is predicted and quantified by linear and weakly nonlinear analyses. The nucleation and growth of a C-SWNT at the center of convection cell is explained.

PACS numbers: 61.46.+w, 47.20.Dr, 47.54.+r, 82.60.Qr

This Letter presents a model which describes the mechanism for the nucleation and growth of carbon single-wall nanotubes (C-SWNTs). Several models have been proposed in the literature [1, 2, 3, 4]; they have succeeded in describing the general scenario leading to growth of C-SWNTs. Our model, however, is able to explain specific and important aspects such as the nucleation, the individual structure of C-SWNTs and their diameter. In brief, our model explains how: 1. the synthesis conditions for C-SWNTs lead to the formation of carbide-metal nanoparticles surrounded by a layer of liquid supersaturated in carbon; 2. a Bénard-Marangoni instability is generated in this liquid layer; 3. the Bénard-Marangoni instability leads to the formation of hexagonal convection cells, at the center of which nanotubes nucleate; 4. the C-SWNTs grow by a root-growth mechanism at least initially and 5. the BMI offers a simple kinetic explanation for the diameter of the C-SWNTs.

Recently, a review of the nucleation and growth of C-SWNTs [5] suggested that an interface instability is responsible for the nucleation of C-SWNTs. Leveraging this idea, we develop a model based on the Bénard-Marangoni instability (BMI), called the BMI model. In this Letter, we show that nucleation of C-SWNTs indeed results from the onset of the BMI. For concreteness, we study the common case of a long bundle growing on one side of a large (5nm to 20nm) nanoparticle (NP) and only consider an iron catalyst, which is known to result in synthesis of C-SWNTs [6]. The treatment remains valid for any catalyst.

We first describe the formation of the nanoparticle and the liquid layer surrounding it, by analysing the iron and carbon (Fe-C) phase diagram (Fig.1). In gas-phase processes, the synthesis begins by the creation of a mixture of Fe-C vapors in an inert gas. The Fe-C mixture is initially at a high temperature (5000°C) (point P0 in Fig.1) and contains a fraction of about 2%-3% of iron atoms with respect to carbon atoms. The vapor mixture is then cooled

very rapidly ($\approx 10^6$ °C/s). As the temperature decreases to around 2300°C (P0 to P1 in Fig.1), the vapor mixture condenses to form nanometric droplets of an iron-carbon solution having a concentration of about 25%-30%at. If the cooling rate remains high, the iron-carbon droplets undergo a non-equilibrium solidification process down to around 1500°C, maintaining droplets in a supersaturated state (P1 to P2 in Fig.1). Subsequently, droplets experience a rapid segregation process [3] so as to recover their equilibrium state. At this point, the carbon concentration in the droplet is higher than the equilibrium liquidus value. As a consequence, carbon is expelled radially toward the surface of the droplet, until the composition of the droplet center reaches the liquidus equilibrium. From this point, the core of the droplet follows a different path in the phase diagram than the layer surrounding this core.

We now discuss the evolution of the droplet core. This core solidifies at the eutectic temperature, T_{eut} (P2 to P3 in Fig.1), by a eutectic transformation that results in the formation of a carbide (Fe_3C) phase and of a $\gamma - Fe$ phase. In agreement with this analysis, the presence of a thin carbide layer has already been observed [1, 4] by transmission electron microscopy at the surface of the core. The analysis is further supported by Saito [1] and Alvarez *et al.* [7], who showed that the synthesis temperature of C-SWNTs and their growth are correlated to the catalyst-carbon eutectic temperature.

In the outer layer of the droplet, the expelled carbon will not have enough time to nucleate into small graphitic flakes. Carbon remains dissolved in atomic form in the liquid metal, resulting in the formation of a nanometric liquid layer surrounding the solid core. This liquid layer is supersaturated in carbon [8], with a concentration of as much as 40%-50%at. (P2 to P4 in Fig.1). We note that the liquid phase still exists few hundreds of degrees below T_{eut} [8, 9] since a solution having a non-equilibrium carbon concentration ($> 25\%$ at. for Fe-C, Ni-C and Co-

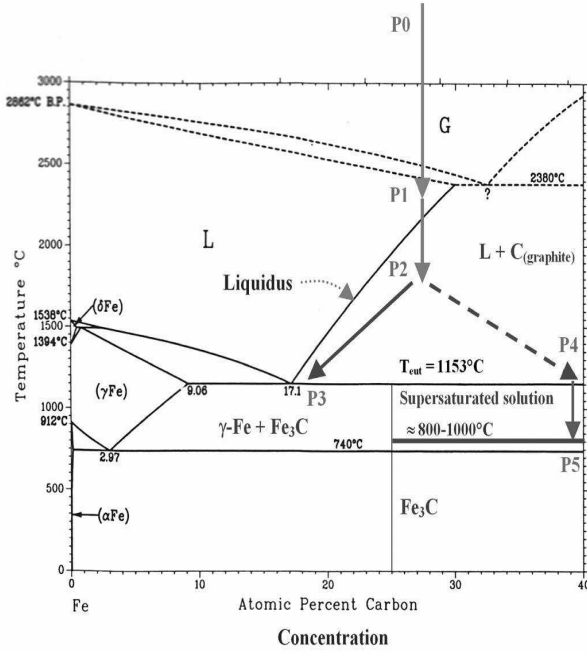


FIG. 1: The overall scenario for growth of C-SWNTs represented in the Fe-C phase diagram

C binary systems) has a lower melting temperature than the eutectic temperature of the system at equilibrium. We can thus define a non-equilibrium eutectic temperature for the supersaturated solution. The melting point of this solution can vary from 800°C to 1000°C and will depend on the carbon concentration, a higher concentration leading to a lower melting point. Therefore, the surface liquid layer can exist from P4 to P5 in the phase diagram Fig.1. This is also supported by Gorbunov *et al.* [2] who proposed that the catalytic nanoparticles involved in the C-SWNTs synthesis are molten.

We now focus on a single NP, and explain a mechanism for the nucleation and growth of nanotubes, driven by a convective instability. A NP is composed of a liquid layer supersaturated in carbon surrounding a solid core composed of a carbide phase and of a $\gamma - \text{Fe}$ phase saturated in carbon. We assume that after the segregation process responsible for the generation of the liquid layer, the concentration in this layer will vary from 25%at. at the solid-liquid interface to 45%at. at the liquid-gas interface. We claim that the Bénard-Marangoni convection governs the carbon transport in the liquid layer. The instability can be driven by temperature or concentration gradients; our calculations will demonstrate that concentration effects dominate.

Since C-SWNTs grow in a bundle from one side of the NP, we neglect curvature effects, and work with a planar geometry. We consider a liquid layer of thickness d and of infinite horizontal extent, with the same carbon concentration gradient as above. The free surface will be considered to be undeformable. Gravity effects can be

neglected because Rayleigh-Bénard convection is negligible compared to the Bénard-Marangoni convection, as will be shown by our calculation. We model the Fe-C solution as a Newtonian and incompressible fluid.

Since the BMI is driven by variations in surface tension σ , which in turn are caused by gradients in concentration \tilde{c} , it is crucial to establish a mathematical relationship between these two quantities. Unfortunately, there is no experimental data available for such non-equilibrium systems. Consequently, we extend the linear dependence $\sigma = \sigma_0 + \gamma_c(\tilde{c} - c_0)$ [10], valid in the eutectic region, to the entire hyper-eutectic region ($\tilde{c} > 17.1\text{at.}$), where carbon acts as a surface tension increasing solute. Here σ_0 and c_0 are the eutectic composition surface tension and concentration, respectively. The solutal surface tension coefficient, γ_c , is assumed constant. We assume the liquid layer is initially in an unperturbed state. The fluid is at rest and the initial concentration profile \tilde{c} is considered linear with respect to the vertical distance Z , $\tilde{c} = c_{SL} + \beta Z$, where β is a (positive) constant concentration gradient and c_{SL} is the carbon concentration at the solid-liquid interface.

The motion of the liquid layer is described by the non-dimensionalized continuity and Navier-Stokes equations:

$$\nabla \cdot \vec{u} = 0, \quad Sc^{-1}(\partial_t \vec{u} + \vec{u} \cdot \nabla \vec{u}) = -\nabla p + \nabla^2 \vec{u}, \quad (1)$$

where (x, y, z) are the three Cartesian coordinates, $\vec{u} = (u, v, w)$ is the velocity, p the pressure, $Sc = \mu/\rho D_L$ the Schmidt number, μ the viscosity, ρ the iron-carbon solution density and D_L the carbon diffusivity in the liquid phase. Here, we have scaled distance, time, velocity, concentration and pressure by d , d^2/D_L , D_L/d , βd and $\mu D_L/d^2$, respectively. We couple the above equations to a solutal diffusion process in the liquid layer modeled by:

$$\partial_t c + \vec{u} \cdot \nabla c = \nabla^2 c - w, \quad (2)$$

where $c = \tilde{c} - \bar{c}$ is the deviation from the unperturbed-state concentration \bar{c} .

At the solid-liquid interface ($z = 0$), the velocity is zero, $\vec{u} = 0$, there is no flux of carbon, $\partial_z c|_{z=0} = 0$, and the carbon concentration is $c_{SL} = 25\text{at.}$ At the liquid-gas interface ($z = 1$), the surface is undeformable, $w|_{z=1} = 0$, and the initial surface concentration of carbon is $c_{LG} = 45\text{at.}$ Depending on the mass transport generated by the solutal BMI, c_{LG} will change with time.

At the onset of the instability, the boundary condition expressing the diffusion of carbon across the surface is given by $\partial_z c|_{z=1} = 0$. As the liquid layer is supersaturated with carbon at the onset of the instability, neither absorption nor adsorption are possible. Thus, the solutal Biot number Bi (characterizing rate of absorption) and the adsorption number Na [11] are both zero.

At the liquid-gas interface, the tangential stress is determined by the surface tension and takes the following nondimensional form:

$$\partial_{zz}w = -Ma_s(\partial_{xx}c + \partial_{yy}c), \quad (3)$$

where the dimensionless solutal Marangoni number

$$Ma_s = \frac{\gamma_c d(c_{LG} - c_{LS})}{\mu D_L}, \quad (4)$$

is an important predictor of the onset of the instability. The critical value of the solutal Marangoni number, Ma_s^c , above which the instability is generated in the case where Na and Bi are zero, is found from previous linear stability analyses [10, 11] to be $Ma_s^c = 50$. We will now show that $Ma_s > Ma_s^c$ under the particular synthesis conditions of C-SWNTs.

We know from experimental observations that the diameter of the core of a NP is generally between 5nm and 20nm [4]. We postulate that the typical thickness of the liquid layer surrounding the core is between 2nm and 4nm. The value of the solutal surface tension coefficient γ_c has been determined in the literature [12] to be $0.03 \text{ N/m} \cdot \%$. We assume that the carbon diffusivity D_L in a highly supersaturated solution is equivalent to substitutional diffusion because interstitial sites are mostly filled. In this case, the diffusivity is almost independent of the nature of the solute for liquid metals and varies between $10^{-9} \text{ m}^2/\text{s}$ and $10^{-8} \text{ m}^2/\text{s}$ [13]. We choose the lower value of diffusion since the liquid layer is supersaturated. Finally, we use a viscosity within the range $\mu = 8 \pm 2 \text{ mPa} \cdot \text{s}$, based on different extrapolations from data [14]. The solutal Marangoni number describing our system is then estimated to be between $Ma_s = 120$ to 400, which is above the critical Marangoni number Ma_s^c required to generate the instability. In contrast, the thermal and solutal Rayleigh numbers and the Marangoni thermocapillary number are estimated to be of the order of 10^{-20} , 10^{-11} and 10^{-3} respectively, far below their respective critical values. It follows from these calculations that the solutal Marangoni effect dominates all the other effects.

Having described the onset of the Bénard-Marangoni instability, we now determine the shape of the convection cells. For this, we rely on the results of the weakly nonlinear analysis done by Bragard *et al.* The parameter necessary to determine the pattern is the distance from the threshold of the instability [10]:

$$\epsilon = \frac{Ma_s - Ma_s^c}{Ma_s^c}. \quad (5)$$

The value of ϵ varies between 1.4 and 7 depending on the thickness of the liquid layer, and can only be considered to be approximate, given the imprecision in the experimental parameters. Using a linear extrapolation (Fig.11

and Table 1 from [10]), we determined the following stable configurations for the convection cells when $Na = Bi = 0$:

Stable configurations	ϵ
Hexagons	$0 < \epsilon < 2.4$
Hexagons, rolls	$2.4 < \epsilon < 6.3$
Rolls, hybrid cells	$\epsilon > 6.3$

We conclude that the hexagonal stable configuration is favoured in the major part of the range of ϵ . Note that we expect rolls and hybrid cells to be unfavorable for the nucleation of C-SWNTs.

We now focus on the nucleation and growth of a C-SWNT at the center of a hexagonal convection cell. There is no mass transport between cells, and therefore it suffices to consider one convection cell. We know from fluid dynamics that in each convection cell, the liquid rises in the center of the hexagon and descends along the edges of the hexagon, forming a vortex ring [15] (Fig. 2a). The center of the top face and bottom face of a cell are stagnation points, where the velocity of the fluid is zero. The stagnation point at the bottom of a cell, lying on the solid-liquid interface, is of crucial importance since we postulate that a C-SWNT nucleates at this point. The tube grows by incorporating carbon atoms from the liquid.

We envision the beginning of the nucleation process as follows: a fraction of the carbon atoms are transported close to the stagnation point on the carbide layer by the convective fluid flow (Fig.2a). The velocity of carbon atoms decreases close to the stagnation point, reducing their kinetic energy to below the adhesion energy on the metal catalyst. There is thus a semi-spherical influence zone around the stagnation point in which carbon atoms move slow enough to be adsorbed onto the catalyst. The semi-spherical shape is imposed by the axial-symmetry of the flow near the center of the cell. This influence zone acts as a heterogeneous nucleation site. Once the carbon is adsorbed at the solid-liquid interface within this zone, it crystallizes under its minimum energy configuration. It has been shown [16] that the nucleation of a closed hemispherical cap is favoured in presence of a metal surface.

As the cap is formed, the topography of the bottom of the cell changes. The stagnation point is lost while a stagnation line (circumference) at the base of the cap is created (Fig. 2b). The shape of the influence zone also changes: it becomes a sector of a torus surrounding the stagnation line (Fig. 2b-c). The hemispherical shape of the cap, observed in experiments [3], guarantees that the angle of contact between the cap and the carbide layer is nearly vertical. Consequently, the carbon atoms decelerate sufficiently and can be incorporated between the cap and the solid surface. The binding of the cap with the metal surface prevents its closure at the bottom

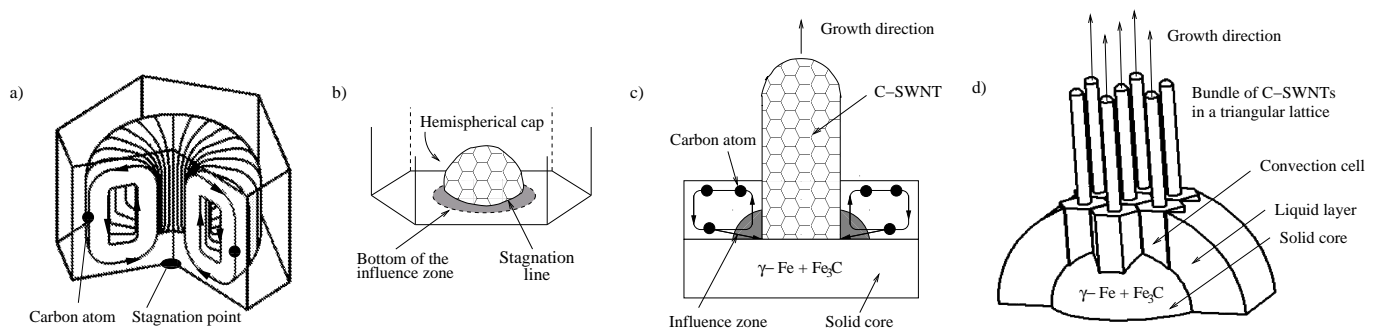


FIG. 2: Steps of the growth: a) Flow in one hexagonal convection cell, b) Formation of a C-SWNT cap on the solid-liquid interface, c) Growth of a C-SWNT in one hexagonal convection cell, d) Collective growth: a bundle of C-SWNTs

and allows the root-growth [3] of a cylindrical structure, the C-SWNT (Fig. 2c). We postulate that the carbon supply at the base of the cap, which is enhanced by the convective flow, exceeds the rate at which bonds in the cap can rearrange. This prevents the lateral growth of the cap and allows the C-SWNT extrusion with a constant diameter [16]. Since the size of a convection cell is known to be of the order of the liquid layer thickness [15], we can estimate the diameter of the C-SWNT to be a few nanometers. This agrees with the diameter of experimentally observed C-SWNTs, (0.7nm-3nm), [3]. Recent total energy calculations using density functional theory predict a larger diameter for the nanotubes, and conjecture a kinetic factor limiting this diameter, [16]. Our BMI model provides precisely such a kinetic explanation. Note that outside the influence zone, it is more favourable for carbon atoms to follow the convection flow than to bind laterally on the C-SWNT since graphitization can only occur at much higher temperatures.

The collection of hexagonal convection cells is responsible for the triangular lattice structure of the bundles of C-SWNTs (FIG. 2d) observed in experiments at the onset of the growth [3]. After the C-SWNTs grow beyond a certain point their organization may be influenced by other factors, but this stage of the growth is outside the scope of our model. Our model explains the nucleation and the beginning of the growth of C-SWNTs in the absence of absorption ($Bi = 0$). However, the carbon atoms initially contained in the liquid layer are not sufficient for the growth of long bundles of C-SWNTs. Carbon atoms must therefore be absorbed from the surrounding gas to maintain the growth process. The extension of the present model to the case when $Bi \neq 0$ is not trivial and will be addressed in a future study.

In summary, using the Fe-C phase diagram, we have explained why a high cooling rate is necessary in the synthesis process to generate a layer of liquid metal sur-

rounding the NP. Leveraging a linear stability analysis, we have shown that the solutal BMI can be generated in the liquid layer. Exploiting a weakly nonlinear analysis, we have shown that the hexagonal pattern can be favoured under the synthesis conditions considered. Once initiated, the BMI is seen to be responsible for the nucleation and growth of C-SWNTs.

* Electronic address: larouche@inrs-emt.quebec.ca

† Electronic address: jonathan.duquette@mail.mcgill.ca

‡ Electronic address: luca.cortelezzi@mcgill.ca

- [1] Y. Saito, Carbon **33**, 979 (1995).
- [2] A. Gorbunov, O. Jost, W. Pompe, and A. Graff, Carbon **40**, 113 (2002).
- [3] J. Gavillet et al., Carbon **40**, 1649 (2002).
- [4] J. Gavillet et al., J. Nanosci. Nanotech. **4** (2004).
- [5] F. L. (to appear), Carbon (2004).
- [6] O. Smiljanic et al., Chem. Phys. Lett. **356**, 189 (2002).
- [7] L. Alvarez et al., Chem. Phys. Lett. **342**, 7 (2001).
- [8] O. P. Krivoruchko and V. I. Zaikovskii, Mendelev Commun. **3**, 97 (1998).
- [9] O. P. Krivoruchko and V. I. Zaikovskii, Kinetics and Catalysis **39**, 561 (1998).
- [10] J. Bragard, S. G. Slavtchev, and G. Lebon, J. Colloid and Interface Science **168**, 402 (1994).
- [11] P. L. T. Brian, AIChE **17**, 765 (1971).
- [12] V. N. Eremenko, *The role of surface phenomena in Metallurgy* (Consultants Bureau enterprises, 1963).
- [13] J.-P. Bâillon and J.-M. Dorlot, *Des Matériaux* (Presse Internationale Polytechnique, 2000, p.204).
- [14] E. T. Turkdogan, *Fundamentals of Steelmaking* (The Institute of Materials, 1996).
- [15] S. Chandrasekhar, *Hydrodynamic and hydromagnetic stability* (International series of monographs on physics, Oxford, England, 1961).
- [16] X. Fan et al., Phys. Rev. Lett. **90**, 145501 (2003).